

Wave run-up on cylindrical and cone shaped foundations for offshore wind turbines

Leen De Vos ^{a,*}, Peter Frigaard ^{b,1}, Julien De Rouck ^a

^a Ghent University, Department of Civil Engineering, Technologiepark 904, 9052 Ghent, Belgium

^b Aalborg University, Department of Civil Engineering, Sohngaardsholmsvej 57, 9000 Aalborg, Denmark

Abstract

During the last decade, several offshore wind-farms were built and offshore wind energy promises to be a suitable alternative to provide green energy. However, there are still some engineering challenges in placing the foundations of offshore wind turbines. For example, wave run-up and wave impacts cause unexpected damage to boat landing facilities and platforms. To assess the forces due to wave run-up, the distribution of run-up around the pile and the maximum run-up height need to be known. This article describes a physical model study of the run-up heights and run-up distribution on two shapes of foundations for offshore wind turbines, including both regular and irregular waves. The influence of wave steepness, wave height and water depth on run-up is investigated. The measured run-up values are compared with applicable theories and previous experimental studies predicting run-up on a circular pile.

The results show that the shape of the foundation substantially affects the maximum run-up level, increasing the expected run-up value. A new relationship between the wave climate (regular and irregular waves) and the run-up is suggested. For this, the velocity stagnation head theory is adjusted and second order Stokes equations are used to calculate the wave kinematics in the crest. The variation of the run-up around the pile is measured and it is found that the position with the lowest run-up level is located under 135° , while the run-up at that position amounts to approximately 40% to 50% of the maximum run-up.

Keywords: Wave run-up; Cylindrical monopile; Conical monopile; Offshore wind turbine; Foundation physical model; Spatial distribution

1. Introduction

During the last decade, several offshore wind-farms were built. Construction of offshore wind turbines encompasses the building of large structures like foundation, pile and turbine. However, there are some smaller installations (boat landing facility, J-Tube, ladder, platform and door) which have to be taken into consideration. Recently, run-up and wave impacts caused damage to existing platform and boat landing facilities. Fig. 1 shows two pictures of wave run-up on one of the wind

turbine foundations of the Horns Rev wind mill farm. The conditions at which the pictures were taken are $H_s=2.5$ m, while the platform level is 9.0 m above SWL. Actual run-up values are much higher than expected or accounted for in the design.

A logical countermeasure against run-up could be to build the platforms on a higher level, where they cannot be reached. However, this brings along other problems. As the wind turbines have to be accessible under all conditions, safety requirements dictate that the distance between boat and platform has to be limited. If these requirements are not met, additional safety measures have to be taken. For example, intermediate platforms are needed when the main platform is placed on too high a level, leading to the initial design problem. Consequently, it is important to have an insight in run-up levels and forces caused by the run-up. Maximum run-up levels determine the design of the platform. Moreover, the run-up distribution around the pile

* Corresponding author. Tel.: +32 9 264 54 89; fax: +32 9 264 58 37.

E-mail addresses: Leen.DeVos@UGent.be (L. De Vos), Peter.Frigaard@civil.aau.dk (P. Frigaard), Julien.DeRouck@UGent.be (J. De Rouck).

¹ Tel.: +45 96 35 80 80.



Fig. 1. Wave run-up on one of the towers of the Horns Rev wind mill farm; $H_s=2.5$ m, platform level=9 m above SWL, *Elsam*.

for the dominant wave direction determines the optimal locations for of boat landing, ladder and door.

This paper presents the results of a small-scale experimental study that examines wave run-up on two different types of pile foundations subject to both regular and random waves. As offshore platforms are placed under diverse conditions, different foundation types are used. It is reasonable to assume that the run-up is influenced by the shape of the foundation. The scale and parameters selected for this study reflect a range useful for understanding the run-up phenomenon on a wind turbine foundation, placed in relatively deep water conditions (17 m to 25 m). A review of applicable theories and previous experimental studies is presented to provide the reader with a clear perspective on how the new test results add to this knowledge base. The main perspective of the paper is to present a clear and easy to use formula to predict wave run-up on wind turbine foundations and to give an estimate of the run-up distribution around the pile.

2. Analytical models for wave run-up

2.1. Velocity stagnation head calculations

Hallermeier (1976) suggests an estimate for run-up by considering the stagnation head at the wave crest as it strikes the cylinder. The assumption is that the water particles at the wave crest are forced to convert their kinetic energy into potential energy by rising a distance equal to $u^2/2g$ up the cylinder above the elevation of the crest. Thus, the run-up is predicted to be

$$R_u = \eta_{\max} + \frac{u^2}{2g} \quad (1)$$

where u =the water particle velocity at the wave crest η_{\max} , both evaluated using some appropriate wave theory.

2.2. Diffraction theory

Linear diffraction theory allows calculation of the wave field around a body of arbitrary shape. This theory is valid for sufficiently small wave heights so linear wave theory is

applicable. The result for the elevation around a circular cylinder surface is (Sarpkaya and Isaacson, 1981)

$$\frac{\eta}{H} = \text{Re} \left[\sum_{m=0}^{\infty} \frac{i\beta_m \cos(m\theta)}{\pi k a H_m^{(1)'}(ka)} \cdot e^{-icot} \right] \quad (2)$$

Where $H_m^{(1)'}$ is a Hankel function of the first kind and

$$\begin{aligned} \beta_m &= 1, \quad m = 0 \\ \beta_m &= 2(-1)^m i^m, \quad m > 0 \\ k &= 2\pi/L, \quad \text{wave number} \end{aligned}$$

The run-up $R_u(\theta)$ around the cylinder is the maximum value of η . Extension of diffraction theory to the second order has been carried out by several other authors (Kriebel, 1990; Martin et al., 2001), using different approaches. These authors have shown that there is a large influence in using a second order theory to calculate run-up and it is not sufficient to attempt an extrapolation based on linear diffraction theory.

As no analytical solution for the maximum value of the expression for η exists, an approximation is used further on in the article. The approximate result for run-up on the up-wave side of a circular cylinder is

$$\frac{R_u}{\eta_{\max}} = \left[1 + \left(\frac{2\pi D}{L} \right)^2 \right]^{1/2} \quad (3)$$

for a cylinder with diameter D .

The threshold of linear diffraction is widely regarded as $D/L > 0.2$. In this range, linear diffraction theory suggests that scattered wave energy is negligibly small. However, this is not the case for steep waves. Experience shows that there are significant nonlinear contributions in the case of steep waves, leading to a considerable amplification of the surface elevation. Stansberg et al. (2005) found that second-order diffraction analysis compare reasonably well in many cases, although there

Table 1
Comparison of experimental studies on wave run-up

Reference	Scatter parameter ka [-]	Deep water wave steepness $\frac{H}{gT^2/2\pi}$ [-]	Relative water depth d/L [-]	Research focus
Niedzwecki and Duggal (1992)	0.11	0.010	0.28	Full length and truncated monopiles; regular and irregular waves
	1.30	0.126	3.32	
Martin et al. (2001)	0.12	0.040	0.28	Monopile; regular waves
	0.32	0.126	3.32	
Mase et al. (2001)	0.08	0.007	0.09	Monopile; regular and irregular waves
	0.24	0.065	0.27	
Current study	0.064	0.016	0.085	Monopile/cone; regular and irregular waves
	1.50	0.10	1.99	

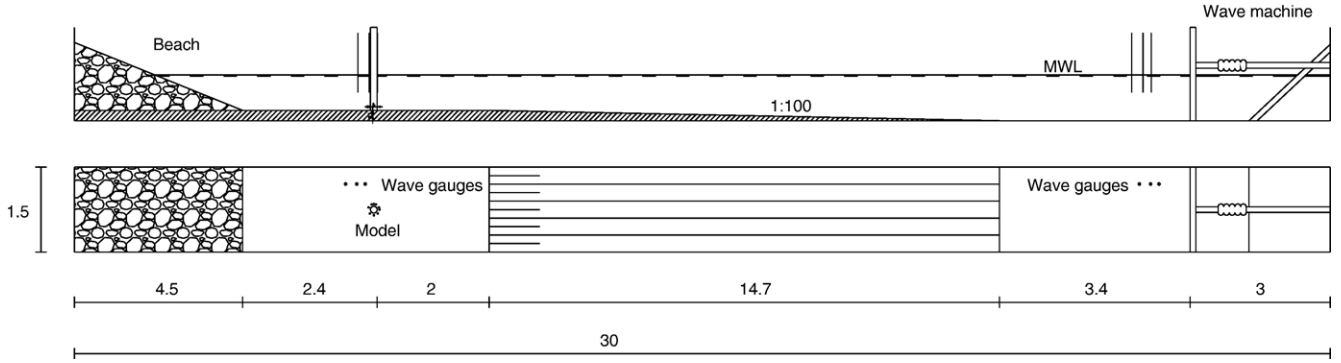


Fig. 2. Test set-up, all values in meters.

are still some discrepancies for steep waves. Fully non-linear modelling is advised in the case of steep waves.

3. Previous experimental studies and semi-empirical run-up formulae

Some previous experimental studies related to the same subject of run-up on piles are shortly described below. If possible, the results of the present experiments are compared with these findings. In Table 1 a comparative view of the dimensionless parameters used in these earlier studies on wave run-up are compared with the parameter range of the current tests.

3.1. Wave run-up and forces on a cylinder in regular and random waves

Niedzwecki and Duggal (1992) performed a small-scale experimental study to investigate wave run-up on rigid full-length and truncated circular cylinders under regular and random sea conditions.

They found that linear diffraction theory underestimates the wave run-up for all but very low wave steepness. When applying the velocity stagnation head theory, Niedzwecki and Duggal used linear theory to calculate wave kinematics and found that run-up heights were under predicted. They employed a semi-empirical variation of the formula, using a coefficient m to be found by fitting a straight line to the data, given by

$$R_u = \frac{H}{2} + m \frac{u^2}{2g} \quad (4)$$

with H the wave height.

They found that on average, $m=6.83$ for a full-length cylinder, while using the maximum horizontal velocity at the still water level.

They found no significant differences for the wave run-up on the truncated and full-length cylinders and conclude that for the considered draft ($d \approx 2D$) the wave run-up is not significantly influenced by the wave kinematics below a certain elevation.

Their experiments were conducted in a flume with dimensions $l \times w \times h = 37 \text{ m} \times 0.91 \text{ m} \times 1.22 \text{ m}$, with a pile diameter of 0.114 m.

They measured the wave elevation over one-half of the cylinder's circumference by five equally spaced resistance type wave gauges, placed directly on the cylinder surface.

In another paper, Niedzwecki and Huston (1992) allow a second coefficient to vary the linear fit, and arrive at

$$R_u = 0.56H + 6.52 \frac{u^2}{2g} \quad (5)$$

for a single cylinder.

3.2. Wave run-up on columns due to regular waves

Martin et al. (2001) investigated run-up on columns caused by steep, deep water regular waves. They compared their experimental results with different theories, including the theories described above (see Section 2) and conclude that most theories underestimate the run-up values. They found that linear diffraction theory is inadequate and used the superposition method of Kriebel (1992), which was still found inadequate for their regime of interest (Table 1), although it did give an improvement of linear diffraction theory. They concluded that the semi-empirical method, suggested by Niedzwecki and Huston overestimates the run-up in nearly all cases.

Their experiments were conducted in a very narrow flume with dimensions $l \times w \times h = 20 \text{ m} \times 0.4 \text{ m} \times 1 \text{ m}$, with a pile diameter of 0.11 m. With a pile diameter to flume width ratio of 0.275, the influence of the side walls on the measurements might be significant. To avoid artificially high blockage in the laboratory model, the value of pile diameter to flume width ratio should be smaller than 0.167 (Whitehouse, 1998). They

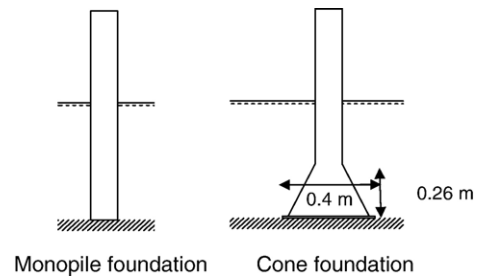


Fig. 3. Monopile foundation, cone foundation.

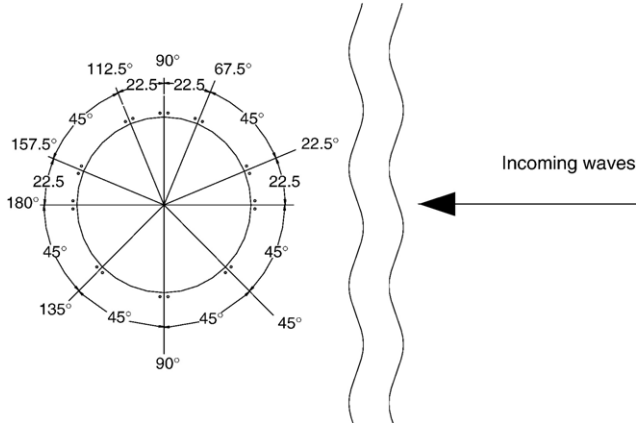


Fig. 4. Position of wave gauges: 10 wave gauges installed 2 mm from the pile surface.

estimated the run-up with visual examination of video recordings.

3.3. Wave run-up of random waves on a small circular pier

Mase et al. (2001) investigated run-up heights of random waves on a small circular pier, installed on a uniform bottom slope, $\tan\theta$, varying between 1:40 to 1:10. They derived a prediction formula for the 2% excess run-up height, as well as the maximum and the one-third maximum run-up heights on a small diameter circular pier as a function of bottom slope $\tan\theta$, deep water wave height H_0 , deep water wave length L_0 and water depth at the pile d . They arrive at the following formula for the 2% run-up (with a correlation coefficient $r=0.98$):

$$\frac{R_{u2\%}}{d} = \left(0.24 - \frac{0.004}{\tan\theta}\right) + \left(11.43 - \frac{0.20}{\tan\theta}\right) \cdot \exp\left[-\left(1.55 - 0.77 \exp\left\{-69.46 \left(\frac{H_0}{L_0}\right)\right\}\right)\right] \cdot \left(1.02 - \frac{0.015}{\tan\theta}\right) \cdot \left(\frac{d}{H_0}\right) \quad (6)$$

They found a linear relationship between the maximum run-up $R_{u\max}$, the significant run-up R_{u_s} and the 2% excess run-up $R_{u2\%}$:

$$R_{u\max} = 1.22 \cdot R_{u2\%} \quad (7)$$

Both formulae are valid for the following conditions:

$$\frac{1}{40} \leq \tan\theta \leq \frac{1}{10}$$

$$0.004 < \frac{H_0}{L_0}$$

$$< 0.05 \frac{d}{H_0} < 6$$

Their experiments were conducted in a flume with dimensions $l \times w \times h = 40 \text{ m} \times 0.7 \text{ m} \times 0.75 \text{ m}$, with a pile diameter of 0.114 m.

They measured the run-up variation by means of a capacitance-type wave gauge, placed 3 mm in front of the structure.

Because the bottom slope at an offshore location of a wind turbine park is often very flat, the present study uses an offshore bottom slope of 1:100, which is much flatter than the bottom slope in the experiments of Mase et al. (2001). Although there is an overlap in most parameters, the comparison of the present test results with the Eq. (6) does not give good results, due to the difference in offshore bottom slope ($\tan\theta=1:40$ to 1:10 as compared to $\tan\theta=1:100$ in this study). This shows that it is recommended to only use the formula of Mase et al. within the specified range.

4. Experimental set-up

4.1. Description of set-up and model

The new experiments are conducted in a wave flume which has a length of 30 m, a width of 1.5 m and a depth of 1 m at Aalborg University, Denmark.

Fig. 2 shows the test set-up. A piston-type wave paddle generates waves at one end of the wave flume, where an absorbing beach is installed at the other end. Two models (Fig. 3) are built in front of the absorbing beach. One model is a monopile foundation, whereas the second model is a cone shaped gravity type foundation. Both models have a pile diameter of 0.12 m. The water depth varies between 0.35 and 0.5 m at the location of the foundation. The offshore slope is fixed at 1:100.

Ten resistance-type wave gauges are mounted on the model to measure the wave run-up and to determine the variation of the run-up around the pile. Fig. 4 shows the position of the wave gauges whereas Fig. 5 shows a picture of the mounted wave gauges.

The wave gauges on the pile are mounted approximately 2 mm from the pile surface. This way it is insured that the water is able to move freely up and down the wave gauges. Marking tapes are placed with a distance of 0.02 m and video recordings are made to allow visual inspection of the recorded run-up measurements.

4.2. Wave conditions

Two different wave types are tested, regular and irregular waves. The target spectrum of the irregular waves is a JONSWAP

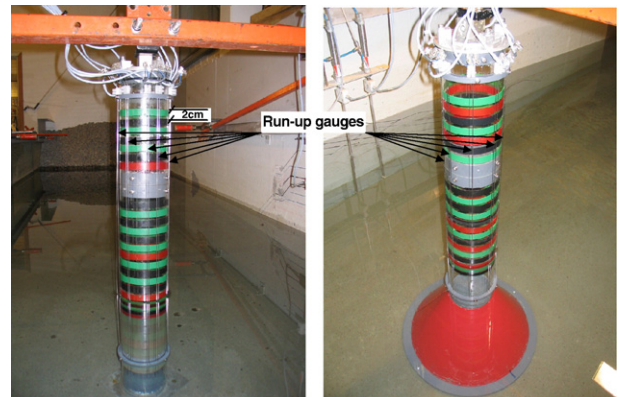


Fig. 5. Mounted capacitance wave gauges on monopile and cone foundation.

spectrum, with a peak enhancement factor γ of 3.3. A total of 60 regular and 36 irregular tests are simulated.

The water surface elevations are measured next to the model with two times three resistance wave gauges. Three gauges are used to separate the incoming and reflected waves by means of the method by [Mansard and Funke \(1980\)](#). Target wave conditions are generated satisfactorily, although slight deviations occur.

The records of irregular waves contain approximately 500 individual waves. The records of regular waves contain approximately 50 waves.

For the regular waves, wave heights vary between 0.01 m and 0.26 m, with a period varying between 0.40 s and 2.78 s, corresponding with a wave steepness varying between 0.02 and 0.12.

For the irregular waves, only larger wave heights (H_s between 0.127 m and 0.224 m) are generated. [Table 2](#) shows the most important parameters for the irregular wave tests. The deep water steepness is defined as $s_0 = H_s / (gT_p^2 / 2\pi)$.

4.3. Definition of run-up

As shown in [Fig. 4](#), 10 resistance wave gauges are mounted on the monopile to measure the run-up distribution around the pile. Run-up is defined as the “green water” level on the surface of the pile. Splash is not taken into account as the wave gauges only measure the green water level. Splash is a phenomenon which occurs mostly with the largest waves. It is assumed that the largest forces on the structure are caused by the green water level.

As mentioned, video recordings were made during the tests. They show that the run-up levels are measured accurately. Only thin run-up layers, caused by the highest waves with very high run-up levels are underestimated slightly due to the distance of wave gauges to the pile (2 mm).

The video images allow differentiating between the run-up caused by breaking waves and the run-up caused by non-breaking waves. They also allow to capture the splash height.

5. Analysis of wave run-up

5.1. Dimensionless quantities

For the irregular waves, it is not obvious what statistical quantity should be used for design. The highest and largest waves cause the largest run-up values, but the thickness of the run-up layer is larger for smaller waves. It is therefore not sure that the highest waves cause the highest load on the deck.

The 2% excess run-up height $R_{u2\%}$ is often used in the studies of run-up on slopes. The use of $R_{u2\%}$ allows a safe design of coastal structures against wave overtopping. [Mase et al. \(2001\)](#) found that the $R_{u\max}$ value only differs by a constant factor from the $R_{u2\%}$ value. They found that $R_{u\max} = 1.22R_{u2\%}$. We found approximately the same value in the present study ($R_{u\max} = 1.23R_{u2\%}$). For this reason only the $R_{u2\%}$ value is studied.

In most theories (valid for regular waves), the run-up is either normalised by the maximum elevation η_{\max} or by the wave height H_{\max} . When using linear theory this leads to $\eta_{\max} = H_{\max} / 2$, but

for a large range of waves (in particular for breaking waves), linear theory is not valid. Therefore beside linear wave theory, also higher order wave theories are used.

5.2. Regular wave test results

Wave height and run-up measurement data are only considered in the steady part of the wave train. [Fig. 6](#) shows an example of a steady part of the wave train, including both the wave signals next to the pile and the simultaneous measurements on all 10 run-up gauges. Even when a steady wave train is reached, slight variations in the waves and in the run-up are observed. To accommodate for the variation, we average 20 consecutive peaks and troughs for the regular wave data. Averaging yields mean values of wave elevation, run-up and run-down. These mean values are plotted in [Figs. 7–14](#).

Some electrical noise on the measured signal is observed. For small wave heights, this signal noise is of the same magnitude as the difference between measured run-up and measured wave height, which might lead to values of $(R_u - H/2)$ smaller than 0. A wave height of 0.14 m yields a noise ratio of

Table 2
Experimental conditions for irregular waves

d [m]	H_s [m]	T_p [s]	$s \left(\frac{2\pi H_s}{g T_p^2} \right)$ [-]	ka [-]	d/L [-]	Models
0.5	0.143	2.10	0.021	0.0877	0.11626	Monopile
0.5	0.159	2.28	0.020	0.0799	0.10603	Monopile Cone
0.5	0.170	2.56	0.017	0.0701	0.09291	Monopile Cone
0.5	0.195	2.56	0.019	0.0701	0.09291	Monopile Cone
0.5	0.199	2.64	0.018	0.0676	0.08969	Monopile
0.5	0.133	1.78	0.027	0.1069	0.14173	Monopile Cone
0.5	0.155	1.95	0.026	0.0957	0.12695	Monopile Cone
0.5	0.165	1.95	0.028	0.0957	0.12695	Monopile Cone
0.5	0.179	2.10	0.026	0.0877	0.11626	Monopile Cone
0.5	0.192	2.10	0.028	0.0877	0.11626	Monopile Cone
0.5	0.127	1.44	0.039	0.1413	0.18741	Monopile
0.5	0.146	1.52	0.041	0.1313	0.17413	Monopile
0.5	0.159	1.61	0.039	0.1218	0.16154	Monopile
0.5	0.167	1.71	0.037	0.1127	0.14943	Monopile
0.5	0.188	1.82	0.036	0.104	0.138	Monopile
0.5	0.112	1.12	0.057	0.2047	0.27147	Monopile
0.5	0.128	1.15	0.061	0.1956	0.25941	Monopile Cone
0.5	0.144	1.30	0.054	0.1629	0.21612	Monopile Cone
0.5	0.158	1.41	0.051	0.1448	0.19202	Monopile Cone
0.5	0.163	1.39	0.054	0.1483	0.19669	Monopile
0.35	0.127	1.67	0.029	0.1328	0.1233	Monopile
0.35	0.133	1.95	0.022	0.1112	0.10321	Monopile
0.35	0.144	2.28	0.018	0.0936	0.0869	Monopile
0.35	0.142	2.10	0.021	0.1022	0.09492	Monopile
0.35	0.145	2.48	0.015	0.0852	0.07908	Monopile

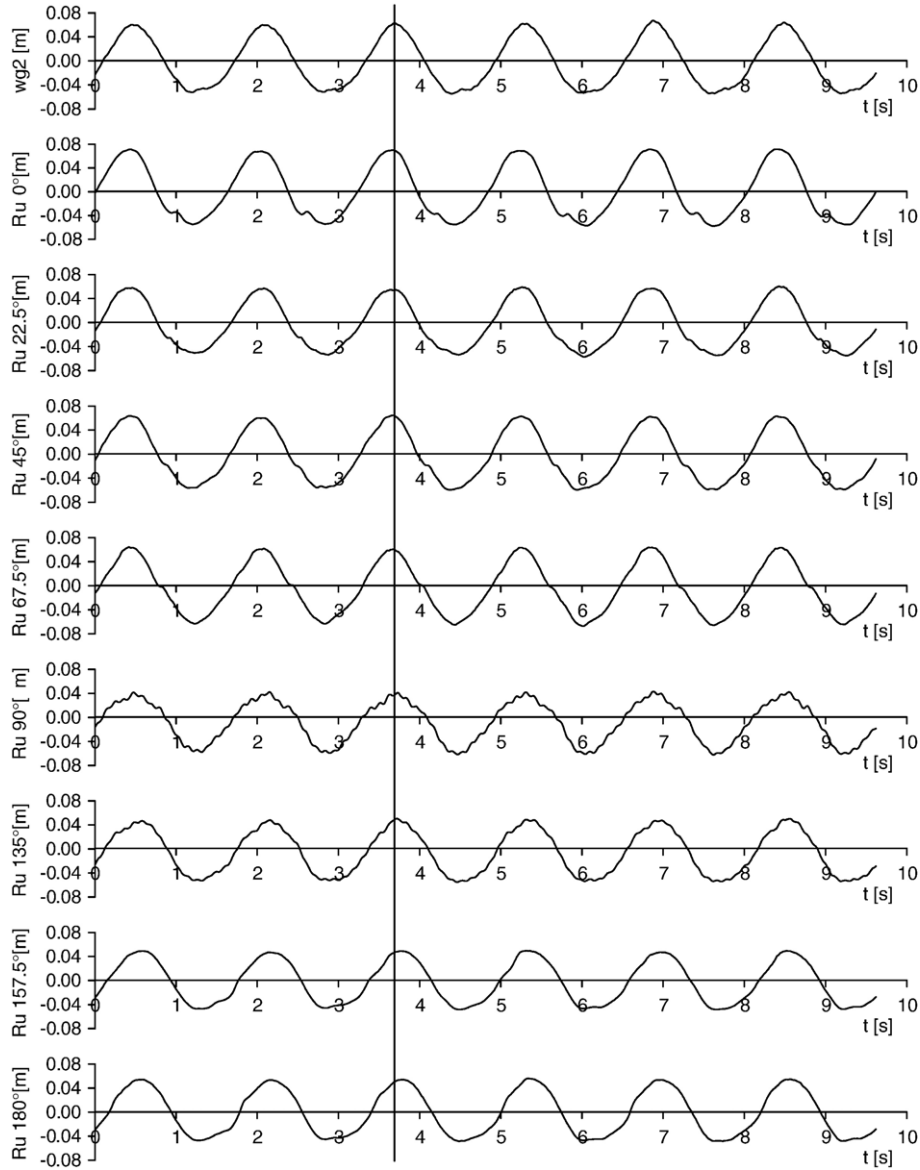


Fig. 6. Steady part of regular wave train ($H=0.12$ m, $T=1.6$ s): wave signal next to the pile ($wg2$) and simultaneous measurements of run-up gauges.

less than 12%. For a wave height of 0.24 m, the noise ratio is already smaller than 2%.

Fig. 7 shows the measured ($R_u - H/2$)-values on the front side of the pile as a function of wave height, for a target deep water wave steepness $s_0=0.03$ (measured deep water wave steepness s_0 varying between 0.24 and 0.34). Overlaid on this graph are three theories using linear wave kinematics and two theories using higher order wave kinematics. Linear theories include the velocity stagnation head theory as well as the suggestions from Niedzwecki and Duggal (1992) and Niedzwecki and Huston (1992). The applied higher order theories are the second order Stokes theory and Fenton's Fourier approximation method.

The graph shows that the velocity stagnation head theory seriously underestimates the run-up value (starting from $H=0.16$ m) when linear theory is applied to calculate the wave kinematics in the crest. The suggestions made by

Niedzwecki and Duggal (1992) and by Niedzwecki and Huston (1992) both overestimate the run-up for smaller wave heights, but for larger wave heights a substantial underprediction is observed. More so, the curve does not reproduce the test results. The occurrence of the measurement at $H=0.26$ m indicates that both theories might seriously underestimate the wave run-up for very high wave heights. Better results are obtained when the velocity stagnation head theory is calculated with higher order (non-linear) wave crest kinematics (assuming that $\eta_{\max} = H_{\max}/2$), as mentioned by other authors (Martin et al., 2001). The applied non-linear theories are the second order Stokes theory and Fenton's Fourier approximation method, with 20 Fourier components. The improvement lies especially in the shape of the curve which follows the trend of the measurements more accurately. $H_{\max}/2$ is used instead of η_{\max} in this representation so that measured run-up values are located above the predictions made by the non-linear theories.

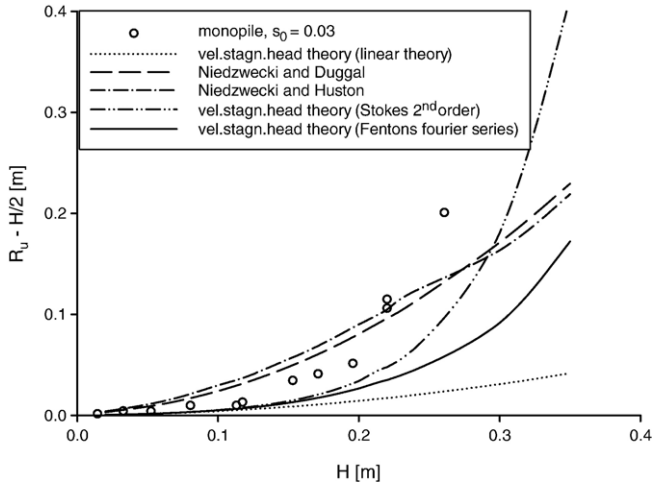


Fig. 7. Run-up on cylindrical monopile for steepness $s_0=0.03$ (regular waves, $d=0.5$ m).

The second order Stokes theory seems to hand good results (bearing in mind that η_{\max} is underestimated by using $H_{\max}/2$ in the velocity stagnation head theory). A huge advantage is that this theory can be solved analytically, while the Fourier approximation method cannot. The implementation of Fenton's theory was done in the program ACES (Automated Coastal Engineering System, 1992).

In Fig. 8, experimental results for different wave steepness are shown. It is difficult to identify from the figure whether the wave steepness has a big influence on the wave run-up, but the highest run-up values are measured for the lowest steepness and run-up values for the highest steepness ($s=0.07$) are somewhat lower than for the other steepness. Linear theory predicts higher run-up values for higher steepness, as u increases when the steepness increases.

Fig. 9 compares the wave run-up on a monopile with the run-up on a cone foundation for regular waves with the same wave steepness. Run-up values for the cone foundation are higher with increasing height of the incident waves.

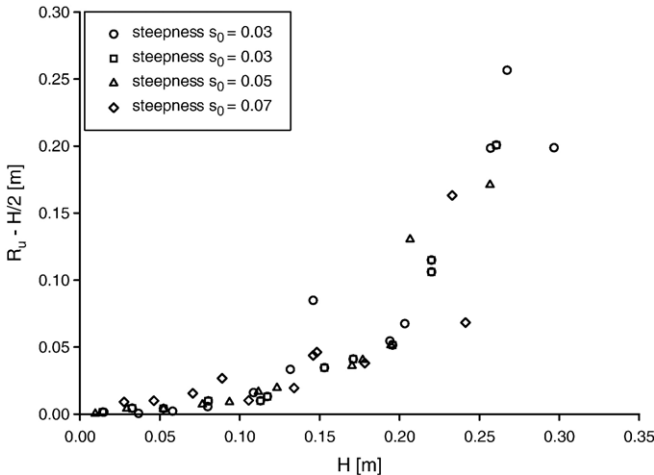


Fig. 8. Run-up on monopile for different wave steepness (regular waves, $d=0.5$ m).

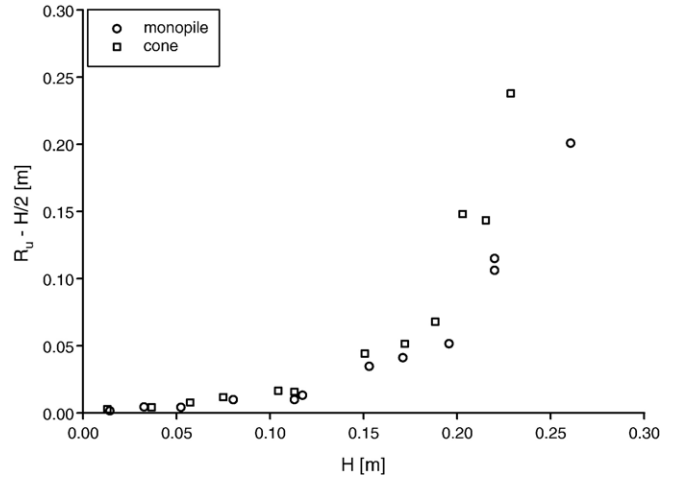


Fig. 9. Run-up on cylindrical and cone shaped foundation for wave steepness $s_0=0.03$ (regular waves, $d=0.5$ m).

In Figs. 10–14 the measured run-up is compared to the estimated run-up for all tests with regular waves, while using the theories which are described in Sections 2 and 3.

In Fig. 10, the velocity stagnation head theory is represented, while linear theory is used to calculate the wave kinematics. Low run-up values are predicted very well, but high run-up values are clearly underestimated.

Fig. 11 shows the prediction made by linear diffraction theory. The run-up prediction shows the same trend as for the velocity stagnation head theory; run-up is seriously underestimated for almost all measured run-up values.

In Fig. 12, the adjustment made by Niedzwecki and Duggal (1992) is presented. In the study of Martin et al. (2001), all run-up values were overestimated by this formula. The present test results show an overestimation of low run-up values, while the high run-up values are underestimated. Further more, it is not possible to get a good estimate of the run-up by adjusting the value of the parameter m in Eq. (4) while using linear theory for

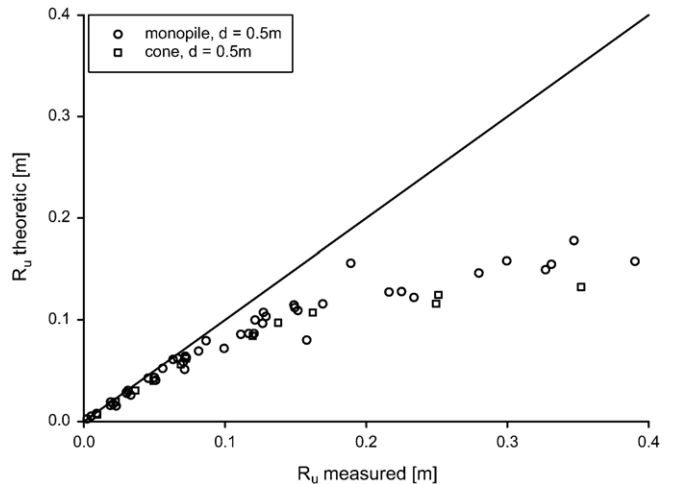


Fig. 10. Comparison between measured and theoretical run-up. Theoretical run-up is calculated using the velocity stagnation head theory (Eq. (1)) with linear theory for wave kinematics (regular waves).

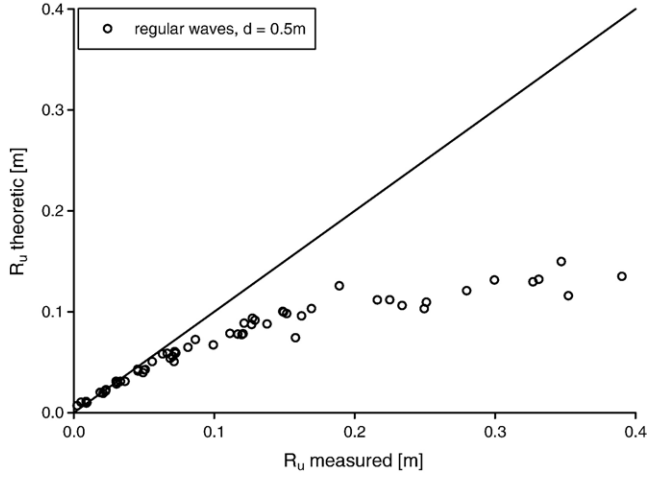


Fig. 11. Comparison between measured (both cylindrical and cone shaped foundation) and theoretical run-up. Theoretical run-up is calculated using the diffraction theory (Eq. (3)) with linear theory for wave kinematics (regular waves).

the wave kinematics. Higher order wave theories offer a better solution.

In Fig. 13, the second order Stokes theory is used to calculate surface elevations:

$$\eta_{\max} = \frac{H}{2} + k \frac{H H \cosh(kd)}{2 \cdot 8 \sinh^3(kd)} (2 + \cosh(2kd)) \quad (8)$$

and the horizontal particle velocity at the wave crest:

$$u_{\text{top}} = \frac{H g k \cosh(k(\eta_{\max} + d))}{2 \omega \cosh(kd)} + \frac{3}{4} k \frac{H^2}{4 \omega} \frac{\cosh(2k(\eta_{\max} + d))}{\sinh^4(kd)} \quad (9)$$

The prediction of the run-up on a monopile is very good, even for large run-up heights. Especially for the lower run-up

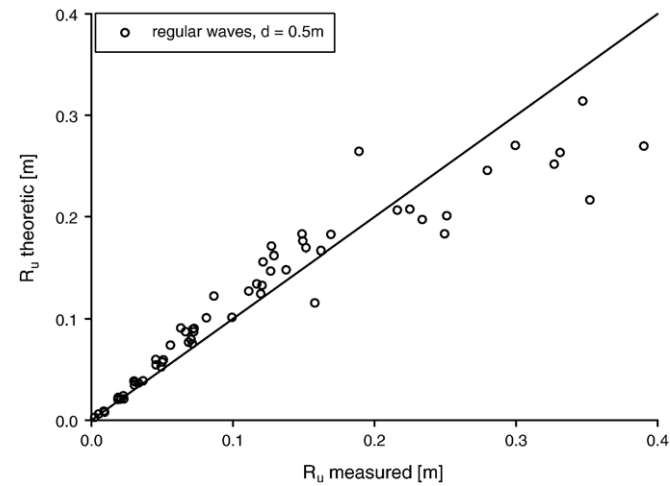


Fig. 12. Comparison between measured (both cylindrical and cone shaped foundation) and theoretical run-up. Theoretical run-up is calculated using Niedzwecki and Duggal's adjustment for the velocity stagnation head theory (Eq. (4), with $m=6.83$) (regular waves).

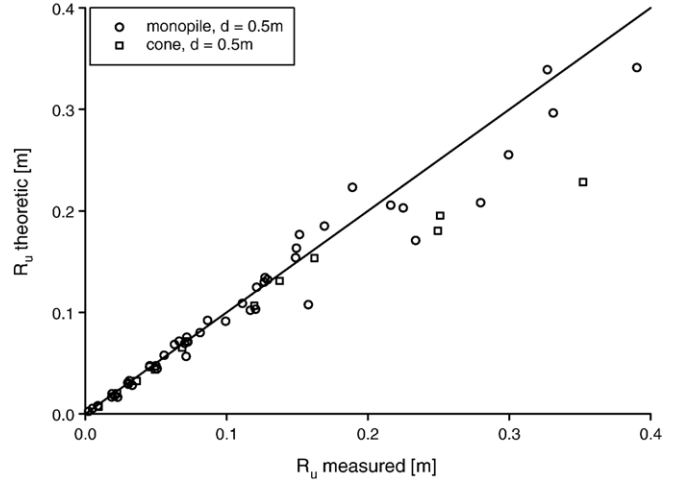


Fig. 13. Comparison between measured and theoretical run-up. Theoretical run-up is calculated using the velocity stagnation head theory (Eq. (1)) with Stokes second order theory for wave kinematics (Eqs. (8) and (9)) (regular waves).

there is a large improvement of the prediction compared to Niedzwecki and Duggal's prediction. For the cone foundation, run-up is underestimated for the larger wave heights.

In Fig. 14, Fenton's Fourier approximation method is used to calculate both η_{\max} and u . The implementation of Fenton's theory was performed using the code of ACES (1992). The run-up prediction is not improved by using this more complicated numerical wave theory.

As the velocity stagnation head theory with wave crest kinematics determined with second order Stokes theory gives the best results, it is further used for the irregular waves. The main goal for the irregular waves is to find a simple reliable formula to calculate the wave run-up.

5.3. Irregular wave experimental results

Although irregular/random waves are often used in the design of offshore structures, there are no simple reliable

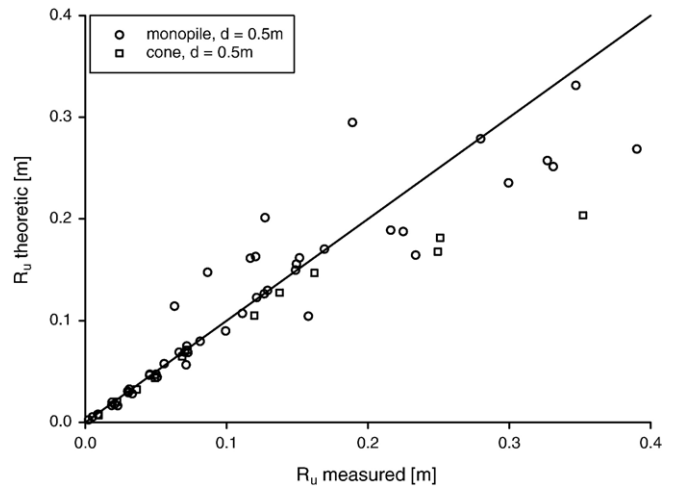


Fig. 14. Comparison between measured and theoretical run-up. Theoretical run-up is calculated using the velocity stagnation head theory (Eq. (1)) with Fenton's Fourier series approximation for wave kinematics (regular waves).

formulae for irregular wave run-up. For this reason, the present study focuses on defining the wave run-up for irregular waves.

A typical part of an irregular wave train is shown in Fig. 15, including both the wave signal next to the pile and the simultaneous measurements on all 10 run-up gauges.

The influence of the wave steepness on the 2% excess run-up is presented in Fig. 16. The target deep water steepness s_0 , presented in this figure, is calculated with H_s and T_p . The measured deep water wave steepness may deviate slightly from the target value. Again, the difference for different wave steepness is limited, but the highest wave steepness (s_0) gives clearly lower run-up values and the highest run-up is measured for the lowest wave steepness.

Fig. 17 shows the 2% excess run-up height as a function of the 2% excess wave height for a monopile in 2 water depths and for the cone foundation. All measurements shown in this figure

have a deep water target wave steepness $s_0=0.03$. Run-up is significantly higher (15 to 35%) for the cone foundation. Due to the limited water depth, wave breaking occurs for $d=0.35$ m, leading to an equal $H_{2\%}$ value for each test. This implies that wave steepness decreases with increasing wave period. Again lower steepness leads to higher run-up values.

For the irregular waves, a spectral analysis of both the run-up and the wave properties can be made (e.g. Niedzwecki and Duggal, 1992). Another possibility is to use linear random wave theory in the case of irregular waves to determine the wave kinematics. The random wave theory decomposes the irregular wave spectrum into component waves and superposes the kinematics determined by linear extrapolation or with stretching techniques such as Wheeler stretching (Randall et al., 1993). Another technique used for the prediction of irregular wave kinematics is to substitute an equivalent regular wave and treat it

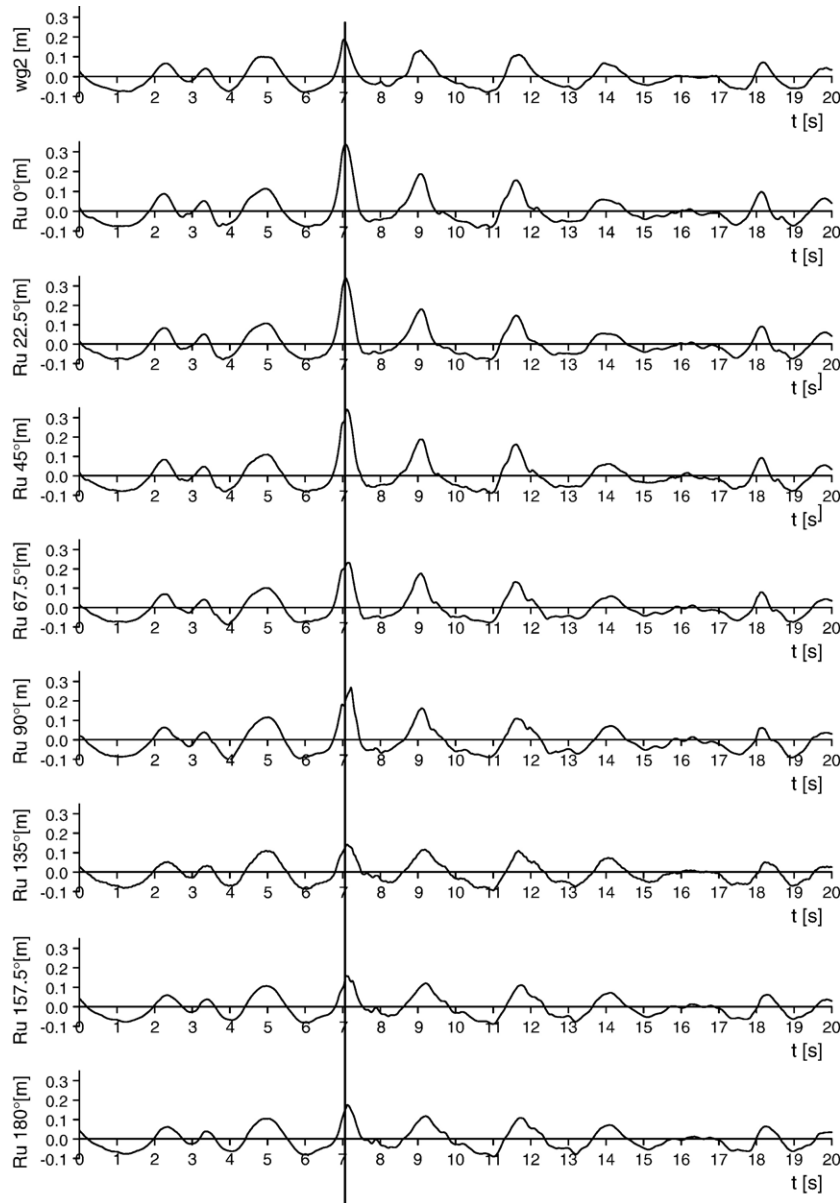


Fig. 15. Irregular wave train ($H_s=0.19$ m, $T_p=2.1$ s): wave signal next to the pile (wg2) and simultaneous measurements of run-up gauges.

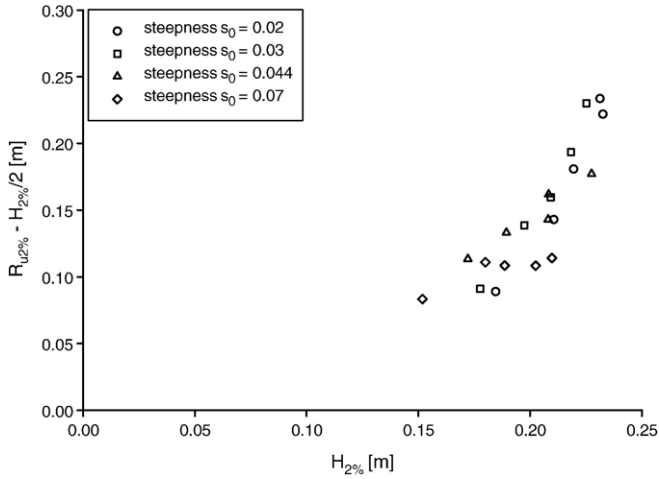


Fig. 16. 2% Excess run-up on monopile for different wave steepness s_0 (irregular waves, $d=0.5$ m).

as a regular wave of equal height and frequency. The wave kinematics can then be computed using a high order non-linear wave theory, such as Stokes theory, and the resulting kinematics are assumed to be that of the irregular wave (Randall et al., 1993). In this study the latter method is used for several reasons. First of all, a comparison between Figs. 16 and 17 and Figs. 8 and 9 reveals a similar behaviour for the wave run-up caused by regular and irregular waves. Secondly, Randall et al. (1993) show that Stokes second order theory gives comparable results to the Wheeler stretching technique for the velocities in the wave crest. They found that where Wheeler stretching under predicts the velocities in an irregular wave and linear extrapolation over predicts the velocities in an irregular wave, Stokes second order theory tends to over predict the velocities under the SWL and slightly over predict the velocities above the SWL. The main reason why the technique of an equivalent regular wave is used, is that it makes it possible to obtain a simple formula.

Using $H_{2\%}$ as a characteristic wave height to predict the 2% run-up value might seem logical. Often however, only limited

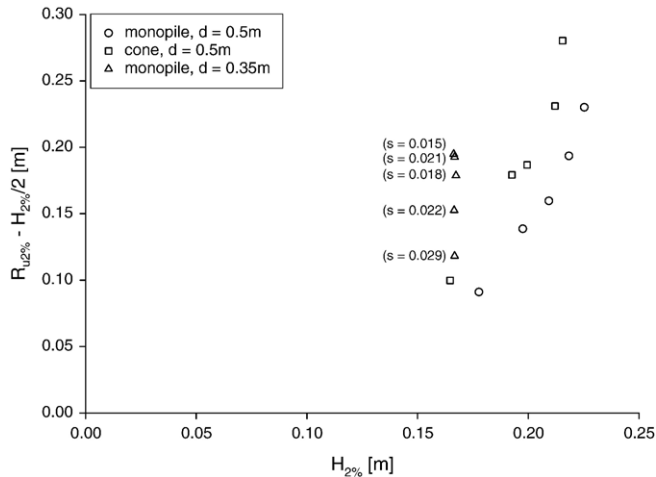


Fig. 17. 2% Excess run-up on different foundations, target wave steepness $s_0=0.03$ (irregular waves).

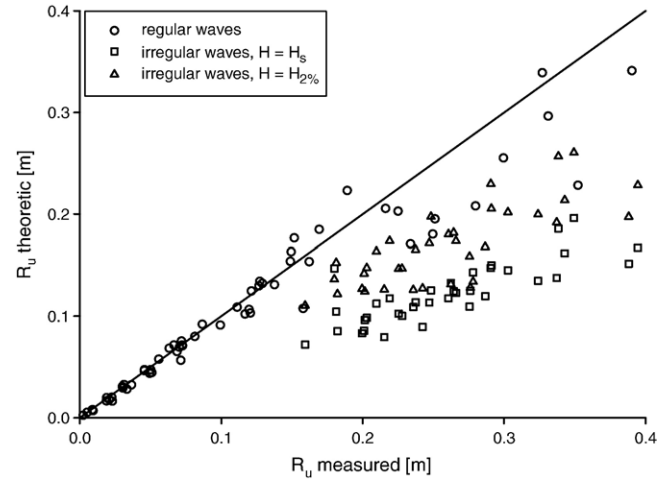


Fig. 18. Comparison between measured and theoretical $R_{u2\%}$. Theoretical run-up is calculated using the velocity stagnation head theory (Eq. (1)) with Stokes second order theory for wave kinematics in the crest (Eqs. (8) and (9)).

wave characteristics (e.g. H_s) are known. For this reason both the significant wave height H_s and the 2% excess wave height $H_{2\%}$ are used to predict wave run-up. T_p is used as a characteristic wave period.

In Fig. 18, the results for the velocity stagnation head theory are shown, applying Stokes second order equations to calculate the wave kinematics in the crest (Eqs. (8) and (9)). The best fit is obtained for the regular waves. For the irregular waves, the theoretic run-up calculated with H_s and $H_{2\%}$ is compared to the measured 2% run-up value. When H_s is used to calculate $R_{u2\%}$, the run-up is seriously underestimated, due to the fact that a much smaller wave height than the one causing the run-up is used. When $H_{2\%}$ is used to calculate the run-up, the estimate is better, but still underestimating the 2% excess run-up.

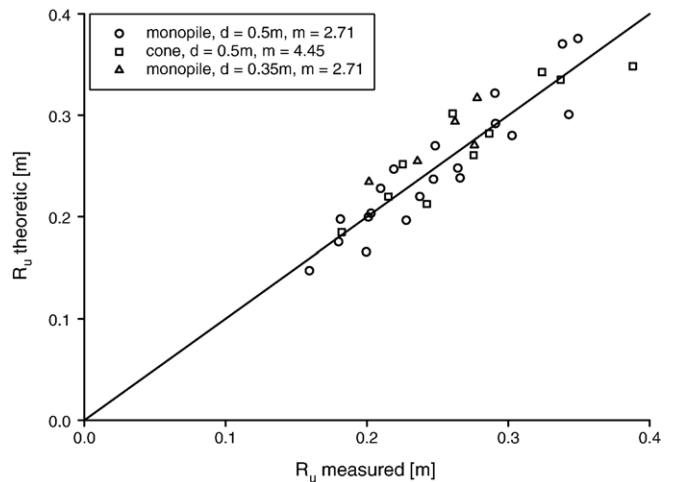


Fig. 19. Comparison between measured and theoretical $R_{u2\%}$. Theoretical run-up is calculated using the adjusted velocity stagnation head theory with Stokes second order theory for wave kinematics in the crest (Eqs. (10) and (11); (irregular waves, $H=H_{2\%}$, $T=T_p$)).

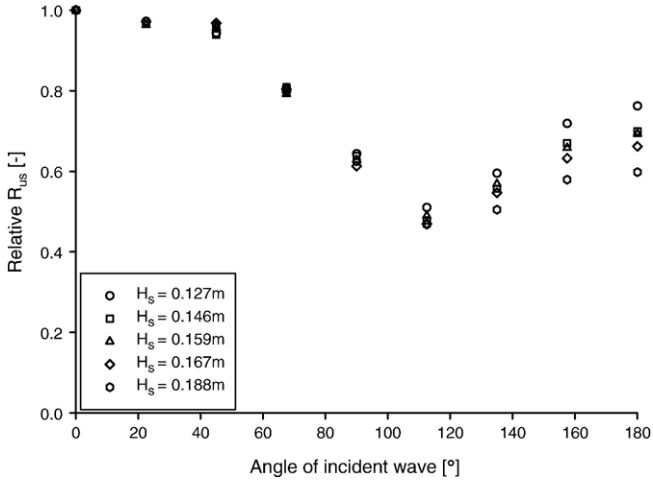


Fig. 20. Variation of significant run-up along the monopile, $s_0=0.044$.

The velocity stagnation head theory is adjusted with a coefficient m in Eq. (4) as suggested by Niedzwecki and Duggal (1992) to improve the results, while using the second order Stokes theory for the wave kinematics. Eqs. (10) and (11) give the best result when η_{\max} is calculated with Eq. (8) and u is calculated with Eq. (9), both using $H=H_{2\%}$ and $T=T_p$. The results are presented in Fig. 19. The value of m is determined by postulating $\overline{R_{u2\%}}_{\text{measured}} = \overline{R_{u2\%}}_{\text{theoretic}}$. As higher run-up values were found for the cone foundation, a different coefficient m is found while trying to find the best fit. We find a value of $m=4.45$ for the cone foundation, while $m=2.71$ for the monopile. The difference indicates that the coefficient m is probably a function of the shape of the foundation and/or the pile diameter. It is however difficult to include this into the parameter m as only two different shapes are tested.

A standard deviation of 0.024 is obtained for all estimates of $R_{u2\%}$, being less than 10% of $\overline{R_{u2\%}} = 0.26$ m.

Eq. (10) is to be used to calculate $R_{u2\%}$ on a monopile foundation:

$$R_{u2\%} = \eta_{\max} + 2.71 \frac{u^2}{2g} \quad (10)$$

For the specific case of the cone foundation, the equation becomes:

$$R_{u2\%} = \eta_{\max} + 4.45 \frac{u^2}{2g} \quad (11)$$

In each of these equations, $H_{2\%}$ and T_p are used to calculate the wave kinematics by means of Eqs. (8) and (9). In most practical cases however, only H_s is known. When the waves are Rayleigh distributed, $H_{2\%}$ can be estimated by

$$H_{2\%} = 1.40H_s \quad (12)$$

One must however be careful to use Eq. (12). When H_s is on the limit of wave breaking, the run-up will be seriously overrated by using both formula (10) and (12).

In the present study, the smaller wave heights are Rayleigh distributed. For the larger significant wave heights, the distribution deviates quite a lot from the Rayleigh distribution due to wave

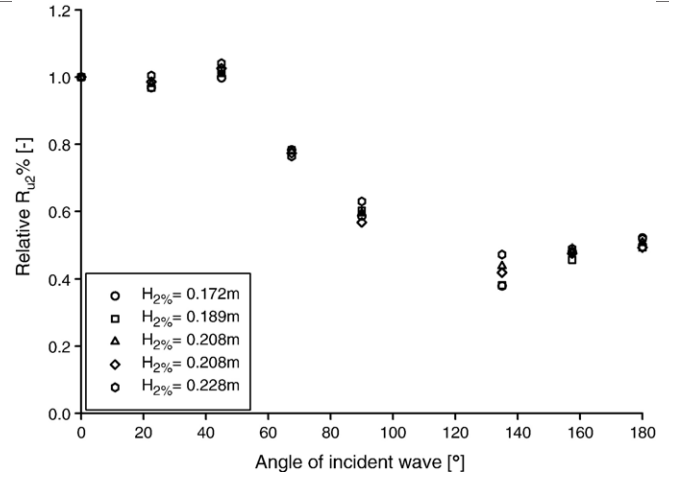


Fig. 21. Variation of 2% run-up along the monopile, $s_0=0.044$.

breaking. In shallow water, Glukhovsky's (1966) distribution can be used. The distribution of the wave heights in the present study tends to be even steeper than Glukhovsky's distribution.

Generally, the Rayleigh distribution is adequate, except for near-coastal wave records in which it may overestimate the number of large waves. Investigations of shallow-water wave records from numerous studies indicate that the distribution deviates from the Rayleigh distribution, and other distributions have been shown to fit individual observations better (SPM, 1984). The primary cause for the deviation is that the large waves suggested in the Rayleigh distribution break in shallow water. Unfortunately, there is no universally accepted distribution for waves in shallow water. As a result, the Rayleigh distribution is frequently used with the knowledge that the large waves are not likely to occur (CEM, 2002).

5.4. Variation of run-up around the pile

The variation of the run-up around the pile for irregular waves was measured at nine different angles of the wave

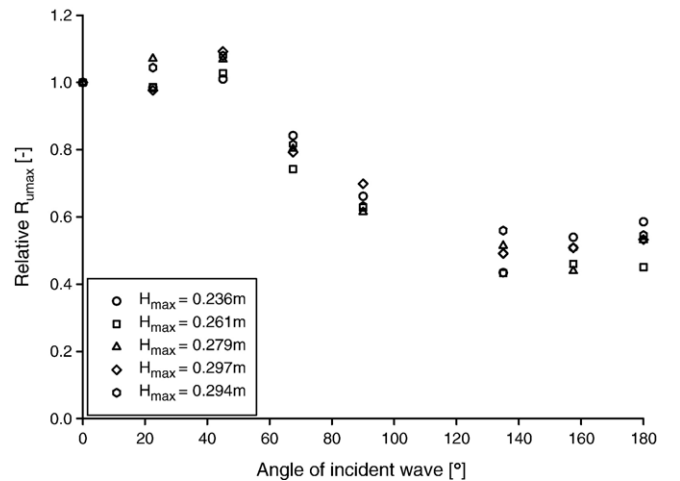


Fig. 22. Variation of maximum run-up along the monopile, $s_0=0.044$.

attack for four different wave steepnesses (0.020, 0.030, 0.044 and 0.070). Figs. 20, 21, and 22 correspond with the measured R_{us} , $R_{u2\%}$ and R_{umax} values relative to the value of the run-up at the front side of the pile, for a wave steepness of 0.044. The relative run-up distribution along the pile is almost independent of the generated wave height. The further from the front line, the more the wave height affects the distribution of the run-up. At the back side of the pile, the relative significant run-up values tend to be smaller for higher waves (Fig. 20). For the 2% run-up and the maximum run-up this is not the case: there seems to be no straightforward relation between the relative run-up at the back side of the pile and the wave height.

When looking at the significant wave height, the maximum run-up is found at the front of the pile. For the 2% and the maximum values, the maximum run-up is mostly found at an angle of 45° . At this location, the measured run-up values are 1% to 9% higher than those at the front side of the pile. The difference increases for the higher waves. This is probably due to the fact that the run-up tongue for very high waves is thinner at the front side of the pile than at an angle of 45° . Due to the distance of the wave gauges to the pile (2 mm), the very thin run-up tongues induced by very high waves are slightly underestimated.

Fig. 21 shows that the lowest 2% run-up is not located on the leeside, as one might expect, but at an angle of approximately 135° . For the significant wave height, the lowest run-up is located at an angle of approximately 122.5° . The run-up at this position amounts to approximately 40% to 50% of the maximum run-up. As the location of the access facilities is optimal where maximum run-up is at its lowest, this information can be combined with information on wave directions to find an optimum location for the access facilities to the wind turbine.

6. Summary and conclusion

Wave run-up on offshore wind turbine foundations is much higher than often predicted by linear wave theory, causing problems for the access facilities. A possible countermeasure exists in placing the platforms higher, preventing the up-running waves to reach them.

In this paper, formulae (Eqs. (10) and (11)) are given to predict wave run-up for irregular waves, based on a small-scale experimental study that examines both regular and irregular wave run-up on two different shapes of pile foundations: cylindrical and conical. The parameters selected for this study reflect a range useful for understanding the run-up phenomenon on a wind turbine foundation, placed in deeper water conditions ($d/L=0.10-0.8$), with a flat bottom slope ($\tan\theta=1:100$). As experience shows and as the formulae predict, run-up can often be so high that placing the platform on a level were it cannot be reached by the waves is hardly manageable. Designers of offshore foundations should therefore take the wave forces from up-running waves into consideration. To obtain the prediction formula for the run-up caused by irregular waves, the velocity stagnation head theory is adjusted with a coefficient m as

suggested by Niedzwecki and Duggal (1992), while using the second order Stokes theory for the wave kinematics. It was found that the shape of the foundation influences the expected run-up level, leading to a different value m for a cylindrical foundation and for the cone foundation. More research is needed to assess the run-up for other foundation shapes and types.

To find an optimal location for the access facilities of the wind turbines, the variation of the run-up around the pile was measured. The test results show that the position with the lowest run-up level $R_{u2\%}$ or R_{umax} is located under 135° , while the run-up at that position amounts to approximately 40% to 50% of the maximum run-up at the frontline.

Acknowledgement

The grant for this research was partially provided by the Research Foundation — Flanders. The Research Foundation — Flanders is gratefully acknowledged.

Appendix A. Appendix: Notation

The following symbols are used in this paper:

a	Cylinder radius
d	Water depth
D	Pile diameter
g	Gravitational acceleration
h	Height of wave flume
H	Wave height
H_s	Significant wave height
H_0	Deep water wave height
$H_{2\%}$	Wave height exceeded by 2% of the waves
k	Wave number
l	Length of wave flume
L	Wave length
L_0	Deep water wave length
m	Coefficient
R_u	Run-up on up-wave side of structure
R_{us}	Significant run-up height
R_{umax}	Maximum run-up height
$R_{u2\%}$	2% excess run-up height
$\overline{R_{u2\%}}$	Average of run-up values higher than the 2% excess run-up height
$\overline{R_{u2\%, measured}}$	Average measured run-up height
$\overline{R_{u2\%, theoretic}}$	Average theoretical run-up height
s	Wave steepness, H/L
s_0	Deep water wave steepness, $2\pi H/gT^2$
T	Wave period
T_p	Peak wave period
u	Horizontal component of wave velocity
w	Width of wave flume
$\tan\theta$	Bottom slope
β_m	Coefficient
η	Water surface elevation
η_{max}	Maximum water surface elevation
ω	Radian wave frequency, $2\pi/T$

References

- Aces, Automated Coastal Engineering System, 1992. Coastal Engineering Research Center, Department of the Army, Mississippi, version 1.07.
- Coastal Engineering Manual, 2002. Part II Chairman Demirbilek Z., Coastal hydrodynamics Chapter II-1, Engineer Manual 1110-2-1100, U.S. Army Corps of Engineers, Washington, D.C. (in 6 volumes).
- Glukhovskiy, B.H., 1966. Investigations of Wind Waves. Gidrometeoizdat Publisher. 284p.
- Hallermeier, R.J., 1976. Nonlinear flow of wave crests past a thin pile. *Journal of the Waterways, Harbors and Coastal Engineering Division* 102 (4), 365–377.
- Kriebel, D.L., 1990. Nonlinear wave diffraction by vertical circular cylinder. Part I: diffraction theory. *Ocean Engineering* 17, 345–377.
- Kriebel, D.L., 1992. Nonlinear wave interaction with a vertical cylinder. Part II: Wave runup. *Ocean Engineering* 19 (1), 75–99.
- Mansard, E.P.D., Funke, E.R., 1980. The measurement of incident and reflected spectra using a least square method. Proc. 17th Coastal Engineering Conference, Sydney, Australia.
- Martin, A.J., Easson, W.J., Bruce, T., 2001. Run-up on columns in steep, deep water regular waves. *Journal of Waterway, Port, Coastal, and Ocean Engineering* 127 (1), 26–32.
- Mase, H., Kosho, K., Nagahashi, S., 2001. Wave run-up of random waves on a small circular pier on sloping seabed. *Journal of Waterway, Port, Coastal and Ocean Engineering* 127 (4), 192–199.
- Niedzwecki, J.M., Duggal, S.D., 1992. Wave run-up and forces on cylinders in regular and random waves. *Journal of Waterway, Port, Coastal, and Ocean Engineering* 118 (6), 615–634.
- Niedzwecki, J.M., Huston, J.R., 1992. Wave interaction with tension leg platforms. *Ocean Engineering* 19 (1), 21–37.
- Randall, R.E., Zhang, J., Longridge, J.K., 1993. Laser Doppler anemometer measurements of irregular water wave kinematics. *Ocean Engineering* 20 (6), 541–554.
- Sarpkaya, T., Isaacson, M., 1981. *Mechanics of Wave Forces on Offshore Structures*. Van Nostrand Reinhold Co., New York.
- Shore Protection Manual, 1984. 4th ed., 2 Vol. U.S. Army Engineer Waterways Experiment Station, U.S. Government Printing Office, Washington, DC.
- Stansberg, C.T., Baarholm, R., Kristiansen, T., Hansen, E.W.M., Rortveit, G., 2005. Extreme Wave Amplification and Impact Loads on Offshore Structures. Offshore Technology Conference.
- Whitehouse, R., 1998. *Scour at marine structures*. Thomas Telford.